Loss-resistant state teleportation and entanglement swapping using a quantum-dot spin in an optical microcavity

C. Y. Hu* and J. G. Rarity

Department of Electrical and Electronic Engineering, University of Bristol, University Walk, Bristol BS8 1TR, United Kingdom

(Received 7 September 2010; published 4 March 2011)

We present schemes for efficient state teleportation and entanglement swapping using a single quantum-dot spin in an optical microcavity based on giant circular birefringence. State teleportation or entanglement swapping is heralded by the sequential detection of two photons and is finished after the spin measurement. The spin-cavity unit works as a complete Bell-state analyzer with a built-in spin memory allowing loss-resistant repeater operation. This device can work in both the weak coupling and the strong coupling regime, but high efficiencies and high fidelities are achievable only when the side leakage and cavity loss is low. We assess the feasibility of this device and show it can be implemented with current technology. We also propose optical spin manipulation methods at single-photon levels, which could be used to preserve the spin coherence via spin echo techniques.

DOI: 10.1103/PhysRevB.83.115303 PACS number(s): 03.67.Hk, 42.50.Pq, 78.20.Ek, 78.67.Hc

I. INTRODUCTION

The key resource for quantum communication[1–3] is entangled pairs (EPR pairs) of particles distributed over large distances. Typically photons are used to encode and transport quantum bits (qubits) over long distance due to their relative insensitivity to decoherence. However, the optical channels suffer from exponential loss, and the resulting rate of generation of remote EPR pairs can be vanishingly small. In the last ten years, schemes for extending the range of quantum communication have been proposed[4–15] using quantum teleportation, i.e., state teleportation and entanglement swapping.[2,3] One crucial component for these schemes is efficient Bell-state analysis. The Bell-state analyzer (BSA) makes a joint measurement on an incoming unknown qubit and one particle of an EPR pair and projects the two-qubit state onto one of the four Bell states. Knowing which Bell state they are in allows the state of the remote particle of the EPR pair to be rotated to match the state of the unknown qubit, thus performing state teleportation. If the unknown qubit is one partner in a remote EPR pair, the entanglement now extends between another two remote partner particles, which is entanglement swapping. Simple but inefficient BSAs can be built using linear optics. For polarization-entangled photons, this consists of a 50-50 beam splitter and two polarizing beam splitters (PBSs) based on two-photon interference.[16] This standard optical BSA can identify only two of the four Bell states, so the corresponding teleportation is probabilistic (at most 50% efficient).[17–19] A further more damaging limitation is that this BSA relies on the synchronous arrival of two indistinguishable photons at the beam splitter. Both photons will have suffered loss, and the probability for both arriving at the same time will be the product of these losses, which is typically much less than 50%.

In order to capture and link all photons that arrive at the BSA, a quantum memory is needed with some form of heralding to announce the photon arrival. In this way a photon arriving in one side of the system is stored until another arrives from the other side, at which point the two photons pass to a complete efficient BSA. Multilink systems based on this approach can have a throughput of photons limited only by the losses of a single link independent of the number of links. However, the fidelity of entanglement generated will be limited by the product of the fidelities of the individual links and would eventually drop below the threshold where the entanglement is useful. This can be remedied by integrating entanglement purification into a repeater as first introduced by Briegel *et al.*[6,7] to distribute entanglement with loss now a polynomial function of distance.

In this work, we present a device that incorporates a complete BSA with heralded single-photon memory to provide a loss-resistant repeater. The corresponding quantum teleportation is efficient (or deterministic in the ideal case), heralded, and loss resistant. The device is based on a charged quantum-dot (QD) carrying a single spin coupled to an optical microcavity and exploits the photon-spin entangling gate that can be achieved in this system.[20–22] This device can be extended to include entanglement purification, and we will report on this aspect elsewhere.[23]

Compared with the standard optical BSAs based on two-photon interference,[16] our BSA has three main advantages: (1) Indistinguishability and synchronization of photons are not required as we exploit the spin coherence rather than the photon coherence. Quantum teleportation is heralded by the sequential detection of two photons at different arrival times and is finished after the spin measurement. (2) It measures all Bell states (is complete) and is loss resistant. Both features, especially the latter, can largely enhance the efficiency. Our BSA has a built-in spin memory, so the time window for it to collect photons is determined by the spin coherence time, which is in the ns or μs range, several orders of magnitude longer than the temporal overlap of photons (typically <10 ps) in standard optical BSAs. As a result, the signal rate or the distance for quantum communication can be significantly enhanced. It is well known that a complete deterministic BSA using linear optics only is impossible.[24] Although complete BSAs using optical[25] or measurement-based[26] nonlinearities are possible, they often suffer from low efficiency. Search for complete and efficient BSAs is always a big challenge in the field of quantum information science.[27–33] The efficiency of our BSA can be 100% in the ideal case and $>35\%$ in a realistic device. We show in this work that this complete and efficient BSA could be implemented with current technology.

(3) It is versatile. Besides BSA, the spin-cavity unit can also work as various entangling gates (e.g., photon-spin, photon-photon, and spin-spin entanglers), photon-spin interface (spin memory), spin-controlled single photon sources, and quantum nondemolition (QND) measurement.[20–22] The compatibility with standard semiconductor processing techniques allows all these functions integrated onto a chip and further scaling up.

The paper is organized as follows: In Sec. II, we discuss the type-I BSA using a single QD spin in a single-sided cavity with its application for state teleportation. In Sec. III, various experimental challenges in implementing this device are discussed. We calculate the BSA fidelity and efficiency in more realistic cavities. Results show that the BSA can work in both the weak coupling and strong coupling regime, but high efficiencies and high fidelities are achieved when the side leakage and cavity loss are low. We also introduce a spin manipulation method using single photons and its potential application to spin echo schemes to prolong the spin coherence time (which limits the storage time of the intrinsic spin memory). In Sec. IV, we show entanglement swapping using the type-I BSA. In Sec. V, the type-II BSA using a single QD spin in a double-sided cavity is presented with its applications for state teleportation and entanglement swapping. Finally, we state our conclusions.

II. BELL-STATE ANALYZER (TYPE I)

The optical selection rule of negatively or positively charged excitons (i.e., the trion X^- or X^+) in QDs enhanced in a cavity-QED system leads to large differences in phase or amplitude of reflection and transmission coefficients between two circular polarizations of photons. This giant circular birefringence (GCB) increases with increasing QD-cavity coupling strength and could be observed in both the strong and the weak coupling regime. The GCB applications for QND measurement, various entangling gates, photon-spin interface, and spin-controlled single photon sources have been discussed in our previous work.[20–22]

Here we consider a QD-confined electron spin in a single-sided microcavity (type I) with the top mirror partially reflective and the bottom mirror 100% reflective. In this spin-cavity system, GCB can manifest as the phase difference in the reflection coefficients between $|R\rangle$ and $|L\rangle$ photons. By suitable detuning of the photon frequency, the phase difference can be adjusted to $\pm\pi/2$, and thus a photon-spin entangling gate can be developed, which is described by a two-qubit phase-shift operator:[20,21]

$$\hat{U}(\pi/2) = e^{i\pi/2(|L\rangle\langle L|\otimes|\uparrow\rangle\langle\uparrow|+|R\rangle\langle R|\otimes|\downarrow\rangle\langle\downarrow|)}, \tag{1}$$

where $|R\rangle$, $|L\rangle$ are right-circular and left-circular photon polarization states, and $|\uparrow\rangle$, $|\downarrow\rangle$ are the spin eigenstates along the optical axis, i.e., photon input and output direction. If the side leakage and loss rate κ_s is lower than the output coupling rate κ, near-unity reflectance can be achieved for the empty cavity at all frequencies and for the trion-coupled cavity around the central frequency region in the strong coupling regime,[20,21] so the gate is deterministic in this ideal case. We will discuss the details in Sec. III.

Note that the two-qubit phase gate $\hat{U}(\pi/2)$ is a kind of conditional phase gate, but not the controlled-Z (CZ) gate, i.e., $\hat{U}(\pi/2) \neq \hat{U}_{\rm CZ}$. This can be easily seen from their matrix representations, which are

$$\hat{U}(\pi/2) = \begin{pmatrix} 1 & 0 & 0 & 0 \\ 0 & i & 0 & 0 \\ 0 & 0 & i & 0 \\ 0 & 0 & 0 & 1 \end{pmatrix} \quad \hat{U}_{\rm CZ} = \begin{pmatrix} 1 & 0 & 0 & 0 \\ 0 & 1 & 0 & 0 \\ 0 & 0 & 1 & 0 \\ 0 & 0 & 0 & -1 \end{pmatrix}. \tag{2}$$

In our case, we define $|R\rangle \equiv |0\rangle$ and $|L\rangle \equiv |1\rangle$ for the photon qubit, and $|\uparrow\rangle \equiv |0\rangle$ and $|\downarrow\rangle \equiv |1\rangle$ for the spin qubit. For our gate, if the input state is $|0\rangle|1\rangle$ or $|1\rangle|0\rangle$, it induces a phase shift of $\pi/2$ on the output state; if the input state is $|0\rangle|0\rangle$ or $|1\rangle|1\rangle$, it has no effect on the output states. For the CZ gate, only if the input state is $|1\rangle|1\rangle$, it induces a phase shift of π on the output state, but has no influence otherwise. Due to the side leakage and the cavity loss, it is hard to achieve a phase shift of π in a realistic cavity-QED system.[34] However, the condition for the $\pi/2$ phase shift is actually achievable in a realistic system with losses as discussed in Sec. III. It is worth pointing out that our phase gate exploits the coherent photon-spin interaction in the linear regime, therefore it is very different from other quantum phase gates based on Kerr nonlinearity in the nonlinear regime.[35–37] Our gate is universal, as discussed in Sec. IV. Recently, Koshino *et al.*[38] proposed the photon-atom SWAP and $\sqrt{\rm SWAP}$ gates based on the photon-atom interaction in a similar system. They worked out these gates in a different way from ours. These gates are also universal, and we believe they have the same functions and merits as the two-qubit phase gate $\hat{U}(\pi/2)$.

First, we show state teleportation with the spin-cavity unit (see Fig. 1). Suppose Alice wants to transfer photon 1 in a unknown state $|\psi^{\rm ph}\rangle_1 = \alpha|R\rangle_1 + \beta|L\rangle_1$ to Bob, and Alice holds the spin-cavity unit. Alice and Bob share a pair of entangled photons 2 and 3 in the state $|\psi^{\rm ph}\rangle_{23} = (|R\rangle_2|L\rangle_3 + |L\rangle_2|R\rangle_3)/\sqrt{2}$ (photon 2 to Alice and photon 3 to Bob). The EPR pair can be generated by either the spontaneous parametric down conversion process,[1] the photon entangler,[21] or the entanglement beam splitter.[22] The electron spin is initialized to $|\psi^s\rangle = (|\uparrow\rangle + |\downarrow\rangle)/\sqrt{2}$. Given the losses

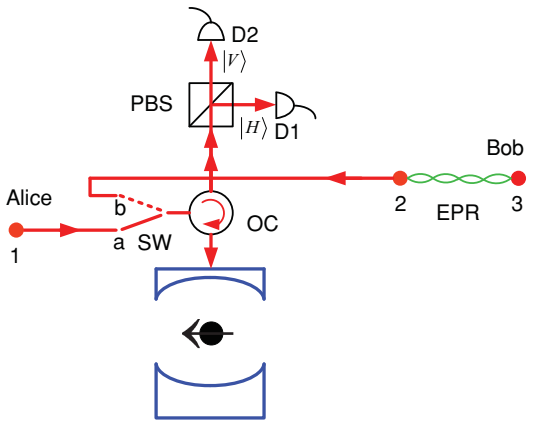

FIG. 1. (Color online) Schematic of state teleportation with a QD-spin in a single-sided microcavity (type I). In this case, the spin-cavity unit works as a three-photon GHZ-state generator and a complete Bell-state analyzer. SW (optical switch), OC (optical circulator), PBS (polarizing beam splitter), D1 and D2 (photon detectors).

the arrival of photon 1 should be heralded before photon 2. Initially an optical switch directs photon 1 from Alice to the system until it is detected in D1 or D2 as shown in Fig. 1. The switch is then switched to await the detection of photon 2. The time difference between photons 1 and 2 should be less than the spin coherence time T_2^e. After the reflection of photons 1 and 2, the total state of three photons with one spin is transformed into

$$|\psi^{\rm ph}\rangle_1 \otimes |\psi^{\rm ph}\rangle_{23} \otimes |\psi^s\rangle \xrightarrow[\text{to photon 1,2}]{\hat{U}(\pi/2)} \times \frac{1}{\sqrt{2}}\{[\alpha|R\rangle_1|R\rangle_2|L\rangle_3 - \beta|L\rangle_1|L\rangle_2|R\rangle_3]|-\rangle + i[\alpha|R\rangle_1|L\rangle_2|R\rangle_3 + \beta|L\rangle_1|R\rangle_2|L\rangle_3]|+\rangle\}, \quad (3)$$

where $|\pm\rangle = (|\uparrow\rangle \pm |\downarrow\rangle)/\sqrt{2}$.

If Alice measured the spin in the $|+\rangle$, $|-\rangle$ basis (e.g., by spin rotations and optical QND measurement),[20,21] the total state would be projected to two partially entangled GHZ states[39] that contain the state information Alice wants to transfer. We see here the spin-cavity unit works as a three-photon GHZ state generator. The spin measurement is not carried out until the detection of photons 1 and 2. By expressing photons 1 and 2 in the $|H\rangle$, $|V\rangle$ basis with a PBS, the right side of Eq. (3) becomes

$$\frac{1}{2\sqrt{2}}\{[|H\rangle_1|H\rangle_2 - |V\rangle_1|V\rangle_2]|-\rangle(\alpha|L\rangle_3 - \beta|R\rangle_3) + i[|H\rangle_1|V\rangle_2 + |V\rangle_1|H\rangle_2]|-\rangle(\alpha|L\rangle_3 + \beta|R\rangle_3) + i[|H\rangle_1|H\rangle_2 + |V\rangle_1|V\rangle_2]|+\rangle(\alpha|R\rangle_3 + \beta|L\rangle_3) + [|H\rangle_1|V\rangle_2 - |V\rangle_1|H\rangle_2]|+\rangle(\alpha|R\rangle_3 - \beta|L\rangle_3)\}. \quad (4)$$

After the photon polarization and the spin measurements, photon 3 at Bob's hand will be found in a state, which is related to the initial state and unequivocally associated to the measurement results consisting of polarizations of photons 1 and 2 in the $|H\rangle$, $|V\rangle$ basis and the spin in the $|+\rangle$, $|-\rangle$ basis (see Table I). By applying the appropriate single-qubit gate[2] on photon 3, Bob gets the initial state Alice wants to transfer. At this point the teleportation procedure is complete.

To investigate the role of the spin-cavity unit further, we consider the two-photon Bell states as the input, i.e., $|\Psi^{\pm}\rangle = (|R\rangle_1|L\rangle_2 \pm |L\rangle_1|R\rangle_2)/\sqrt{2}$ and $|\Phi^{\pm}\rangle = (|R\rangle_1|R\rangle_2 \pm |L\rangle_1|L\rangle_2)/\sqrt{2}$, and get the following transformations:

$$\hat{U}(\pi/2)|\Psi^{\pm}\rangle|+\rangle = i|\Psi^{\pm}\rangle|+\rangle, \quad \hat{U}(\pi/2)|\Phi^{\pm}\rangle|+\rangle = |\Phi^{\mp}\rangle|-\rangle. \quad (5)$$

Obviously, the spin measurements in the $|+\rangle$, $|-\rangle$ basis can distinguish $|\Psi^{\pm}\rangle$ from $|\Phi^{\pm}\rangle$, and the photon polarization measurement in the $|H\rangle$, $|V\rangle$ basis can distinguish between $|\Psi^+\rangle$ and $|\Psi^-\rangle$ and between $|\Phi^+\rangle$ and $|\Phi^-\rangle$. So the spin-cavity unit with a PBS is a complete BSA. If expressing photons 1 and 2 in the $|\Psi^{\pm}\rangle$, $|\Phi^{\pm}\rangle$ basis on the right side of Eq. (3), we get the same result as Eq. (4).

TABLE I. The correspondence between the photon 1, 2 polarization and the spin measurement results and the photon 3 states in the case of the state teleportation.

Photons 1, 2	Spin	Photon 3
$\|H\rangle_1\|H\rangle_2$ or $\|V\rangle_1\|V\rangle_2$	$\|-\rangle$	$\alpha\|L\rangle_3 - \beta\|R\rangle_3$
$\|H\rangle_1\|V\rangle_2$ or $\|V\rangle_1\|H\rangle_2$	$\|-\rangle$	$\alpha\|L\rangle_3 + \beta\|R\rangle_3$
$\|H\rangle_1\|H\rangle_2$ or $\|V\rangle_1\|V\rangle_2$	$\|+\rangle$	$\alpha\|R\rangle_3 + \beta\|L\rangle_3$
$\|H\rangle_1\|V\rangle_2$ or $\|V\rangle_1\|H\rangle_2$	$\|+\rangle$	$\alpha\|R\rangle_3 - \beta\|L\rangle_3$

As the spin-cavity unit also works as a photon-spin interface,[21] our BSA contains a built-in spin memory with the storage time limited by the spin coherence time T_2^e. The above teleportation procedure can be understood in another way: On detecting photon 1, the initial state is transferred to the spin and stored on it; on detecting photon 2, the spin and photon 3 get entangled; after the spin measurement, the state is transferred from the spin to photon 3. As we exploit coherent photon-spin interaction rather than the two-photon interference, our BSA does not require synchronized and indistinguishable photons in contrast to the standard optical BSA.[17–19] The synchronization should be maintained within the photon coherence time (typically <10 ps) for the standard optical BSA, whereas the time window for our BSA to capture photons is equal to the spin coherence time T_2^e. As discussed in Sec. III, the electron spin decoherence time is normally several ns for InAs- or GaAs-based QD when no spin protection methods are applied. In this case, the signal rate for quantum communication using our BSA is enhanced by up to two orders of magnitude,[40] and the distance at the same signal rate (or the length of each repeater segment) is increased by up to five times, compared with that using the standard optical BSA. Using the spin echo techniques (see Sec. III), T_2^e could be extended to the μs range. As a result, the signal rate could be enhanced by up to five orders of magnitude, or the distance by 12 times. Therefore, our BSA can combat losses in quantum channels and holds great potential for long-distance quantum communication.[41–43] For example, the longest distance for quantum communication is currently kept around 100 km. With our BSA, the distance (without the help of quantum repeaters) could be extended to over 1000 km, at which most satellites are covered.[44]

III. EXPERIMENTAL CHALLENGES

In this section, we discuss the feasibility to implement the BSA function in a promising system with GaAs- or InAs-based QDs in micropillar microcavities. This type of microcavity with circular cross-section can support circularly polarized light and have negligible mode mismatching between the traveling and the cavity photons.[45] However, other cavity structures (e.g., that in Ref. 46) can also be suitable for our schemes if the cavities are made symmetric to support circularly polarized light.

To calculate the fidelity and efficiency for the entanglement analysis, we have to use the reflection operator, rather than the phase-shift operator $\hat{U}(\pi/2)$, to describe the photon-spin entangling gate,[20,21] i.e.,

$$\hat{r}(\omega) = r_0(\omega)(|R\rangle\langle R| \otimes |\uparrow\rangle\langle\uparrow| + |L\rangle\langle L| \otimes |\downarrow\rangle\langle\downarrow|) + r_h(\omega)(|L\rangle\langle L| \otimes |\uparrow\rangle\langle\uparrow| + |R\rangle\langle R| \otimes |\downarrow\rangle\langle\downarrow|), \quad (6)$$

where $r_0(\omega) \equiv |r_0(\omega)|e^{i\varphi_0(\omega)}$ and $r_h(\omega) \equiv |r_h(\omega)|e^{i\varphi_h(\omega)}$ are the reflection coefficients for the empty (or cold) cavity (with trion uncoupled to the cavity) and hot cavity (with trion coupled to

the cavity), respectively. In the weak excitation approximation where the real excitation can be neglected,[47] $r_h(\omega)$ and $r_0(\omega)$ are given by[20]

$$r_h(\omega) = 1 - \frac{\kappa\left[i(\omega_{X^-} - \omega) + \frac{\gamma}{2}\right]}{\left[i(\omega_{X^-} - \omega) + \frac{\gamma}{2}\right]\left[i(\omega_c - \omega) + \frac{\kappa}{2} + \frac{\kappa_s}{2}\right] + g^2},$$
$$r_0(\omega) = \frac{i(\omega_c - \omega) - \frac{\kappa}{2} + \frac{\kappa_s}{2}}{i(\omega_c - \omega) + \frac{\kappa}{2} + \frac{\kappa_s}{2}}, \tag{7}$$

where ω, ω_c, ω_{X^-} are the frequencies of input photon, cavity mode, and X^- transition, respectively. g is the coupling strength between X^- and the cavity mode. $\gamma/2$ is the X^- dipole decay rate, and $\kappa/2$, $\kappa_s/2$ are the cavity field decay rate into the output modes and the leaky modes (e.g., side leakage and cavity loss), respectively. The GCB effect comes from $r_0(\omega) \neq r_h(\omega)$ in either the phase or the reflectance. Instead of the dispersive interaction,[48] we consider the resonant interaction with $\omega_c = \omega_{X^-} = \omega_0$ in this work. Note that the reflection operator in Eq. (6) consists of the contributions from both the empty and the hot cavity and is the general and rigorous form from which we derive the phase-shift operator $\hat{U}(\pi/2)$.

If the side leakage and cavity loss rate κ_s is much lower than the output coupling rate κ (the ideal case), we have $|r_0(\omega)| \simeq 1$ at all ω's for the empty cavity, and $|r_h(\omega)| \simeq 1$ around the central frequency regime for the hot cavity in the strong coupling regime. The reflection operator $\hat{r}(\omega)$ in Eq. (6) can be simplified as the phase-shift operator $\hat{U}(\pi/2)$ in Eq. (1) with unity fidelity and efficiency. However, when the side leakage and cavity loss cannot be neglected, the empty and the hot cavity have different reflectance in general, and the gate fidelity and efficiency will be reduced. The fidelity (in amplitude) is given by

$$F^{(\Psi^\pm)} = 1,$$
$$F^{(\Phi^\pm)} = \frac{1}{\sqrt{1 + \frac{1}{4}\left[\frac{|r_0(\omega')|}{|r_h(\omega')|} - \frac{|r_h(\omega')|}{|r_0(\omega')|}\right]^2}}, \tag{8}$$

and the efficiency is

$$\eta = \eta^{(\Psi^\pm)} = \eta^{(\Phi^\pm)} = \frac{1}{4}[|r_0(\omega')|^2 + |r_h(\omega')|^2]^2, \tag{9}$$

where ω' satisfies $\varphi_h(\omega') - \varphi_0(\omega') = \pm\pi/2$. The fidelity to analyze $|\Psi^\pm\rangle$ remains unity, whereas the fidelity to analyze $|\Phi^\pm\rangle$ is generally less than one, depending on how different $|r_0(\omega')|$ and $|r_h(\omega')|$ are. Figure 2 presents the numerical calculations of the BSA fidelity and efficiency by taking the trion decay rate γ several μeV, which is common for InAs- or GaAs-based QDs, and much smaller than the cavity decay rate of interest. The condition of $\varphi_h(\omega') - \varphi_0(\omega') = \pm\pi/2$ can be satisfied at various frequency detunings, leading to multiple fidelity and efficiency curves for each loss ratio κ_s/κ.[49] If $\kappa_s > 1.3\kappa$, the phase shift $\pm\pi/2$ cannot be achieved, and the above discussions are invalid; i.e., the proposed BSA does not work. If $\kappa_s < 1.3\kappa$, a phase shift of $\pm\pi/2$ can be achieved, and the BSA can work in both the strong coupling regime with $g > (\kappa + \kappa_s)/4$ and the weak coupling regime with $g < (\kappa + \kappa_s)/4$. We illustrate this by highlighting points 1–4 in Fig. 2. In the weak coupling regime, we can achieve

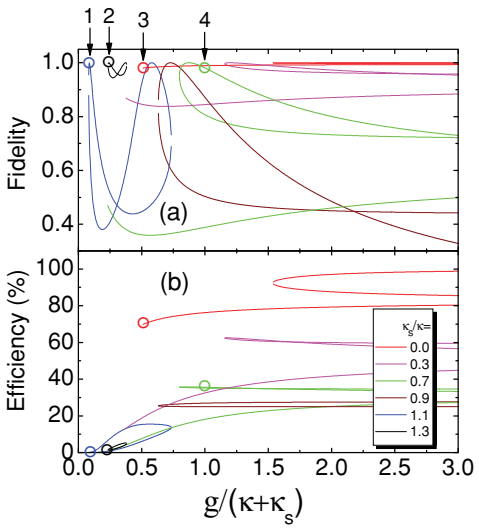

FIG. 2. (Color online) Schematic of state teleportation with a QD-spin in a single-sided microcavity (type I). In this case, the spin-cavity unit works as a three-photon GHZ-state generator and a complete Bell-state analyzer. SW (optical switch), OC (optical circulator), PBS (polarizing beam splitter), D1 and D2 (photon detectors).

unity fidelity, i.e., $F^{(\Phi^\pm)} = F^{(\Psi^\pm)} = 1.0$ at points 1 and 2. However, the efficiency is quite low: $\eta = 0.03\%$ at point 1 where $g/(\kappa + \kappa_s) = 0.086$ and $\kappa_s/\kappa = 1.1$, and $\eta = 1.4\%$ at point 2 where $g/(\kappa + \kappa_s) = 0.24$ and $\kappa_s/\kappa = 1.3$. In the strong coupling regime, both the fidelity and the efficiency can be high. In the ideal case where $g/(\kappa + \kappa_s) > 1.5$ and $\kappa_s/\kappa \ll 1$, near-unity fidelity and near-unity efficiency can be simultaneously achieved, and the reflection operator $\hat{r}(\omega)$ in Eq. (6) can be simplified as the phase-shift operator $\hat{U}(\pi/2)$ in Eq. (1). This case is exactly what we discussed in our previous work.[20,21] Point 3 represents the small loss limit ($\kappa_s/\kappa \approx 0$), where we can achieve near-unity fidelity ($F^{(\Phi^\pm)} = 0.98$, $F^{(\Psi^\pm)} = 1.0$) and efficiency $\eta = 69.9\%$ at $g/(\kappa + \kappa_s) = 0.51$. Also we include point 4, which is experimentally achievable in the strong coupling regime (see the following arguments). At point 4, near-unity fidelity ($F^{(\Phi^\pm)} = 0.98$, $F^{(\Psi^\pm)} = 1.0$) is associated with $\eta = 35.6\%$ efficiency when $g/(\kappa + \kappa_s) \simeq 1.0$ and $\kappa_s/\kappa \simeq 0.7$.

It is easy to achieve the weak coupling experimentally; however, the strong coupling, which is more challenging, has also been observed in various QD-cavity systems,[50–54] and $g/(\kappa + \kappa_s) \simeq 0.5$ was reported[50] for $d = 1.5\,\mu$m micropillar microcavities with a quality factor $Q = 8800$. By improving the sample designs, growth, and fabrication,[53] the quality factors for the micropillars of the same size were increased to $\sim 4 \times 10^4$, corresponding to $g/(\kappa + \kappa_s) \simeq 2.4$ (Ref. 55). However, the quality factors in these micropillars are dominated by the side leakage and cavity loss rate, rather than the output coupling rate,[53] i.e., $\kappa_s/\kappa \gg 1$, which is not what we want. In order to reduce κ_s/κ, we could take such high-Q micropillars and thin down the top mirrors to decrease the quality factor to $Q \simeq 1.7 \times 10^4$. This process increases κ, whereas it keeps κ_s nearly unchanged (or slightly reduced). As a result, we get $\kappa_s/\kappa \simeq 0.7$, whereas the system now with $g/(\kappa + \kappa_s) \simeq 1.0$ remains in the strong coupling regime, corresponding to the

point 4 in Fig. 2. Therefore, the proposed BSA and all related schemes could be implemented with current technology. Small κ_s/κ in the strong coupling regime is highly demanded for high-efficiency operation and could be quite challenging for micropillar microcavities. We notice that recent experiments are quite promising with the strong coupling achieved in large micropillars (7.3 μm diameter),[56] where the side leakage is small compared with small micropillars.

Due to the spin decoherence, the fidelity in Eq. (8) decreases by a factor F',

$$F' = \left[1 + \exp\left(-\Delta t / T_2^e\right)\right]/2, \tag{10}$$

where T_2^e is the electron spin coherence time and Δt is the time interval between two input photons for Bell-state analysis. To get high fidelity, the time interval between two photons should be shorter than the spin coherence time T_2^e, i.e., $\Delta t < T_2^e$. As discussed later, T_2^e could be extended to μs using spin echo techniques. To make the weak excitation approximation valid, Δt should be longer than $\tau/n_0 \sim$ ns,[57] where τ is the cavity photon lifetime and n_0 is the critical photon number of the spin-cavity system.[58]

The trion dephasing can also reduce the fidelity by a factor of τ/T_2, where τ is the cavity photon lifetime and T_2 is the trion coherence time. Two kinds of dephasing processes should be considered here: the optical dephasing and the spin dephasing of X^-. It is well known that the optical coherence time of excitons in self-assembled In(Ga)As QDs can be as long as several hundred picoseconds,[59–61] which is ten times longer than the cavity photon lifetime (around tens of picoseconds in the strong coupling regime for cavity Q-factor of 10^4–10^5). So the optical dephasing can slightly reduce the fidelity by only a few percent. The spin dephasing of the X^- is mainly due to the hole-spin dephasing. In the absence of significant hyperfine interaction that happens for holes due to the p-orbital character,[62,63] the QD-hole spin is expected to have long coherence time,[64,65] and $T_2^h > 100$ ns has been reported recently.[66] This hole spin coherence time is at least three orders of magnitude longer than the cavity photon lifetime, so the spin dephasing of the X^- can be safely neglected in our considerations.

For a realistic QD, the optical selection rule is not perfect due to the heavy-light hole mixing. This can reduce the fidelity by a few percent as the hole mixing in the valence band is in the order of a few percent[67] [e.g., for self-assembled In(Ga)As QDs]. The hole mixing could be reduced by engineering the shape and size of QDs or choosing different types of QDs. Note that our schemes are immune to the fine structure splitting as it occurs for neutral excitons, but not for charged excitons due to the quenched exchange interaction,[68,69] which is in accordance with Kramer's theorem.

Recently, significant progress has been made on optical spin cooling[70,71] and optical spin manipulating[72–75] in QDs. For our schemes, we could alternatively apply the phase gate $\hat{U}(\pi/2)$ to perform single-shot QND measurement and initialize or read out the spin states via single-photon measurement.[20–22] The quantum Zeno effect[76,77] could be used to maintain the prepared states. Spin manipulation is also possible by using the phase gate $\hat{U}(\pi/2)$. One photon in the $|R\rangle$ or $|L\rangle$ state can make 90° spin rotations around the optical axis after the photon is reflected from the cavity with the transformation

$$\begin{aligned} \hat{U}(\pi/2)|R\rangle(\alpha|\uparrow\rangle + \beta|\downarrow\rangle) &= |R\rangle(\alpha|\uparrow\rangle + i\beta|\downarrow\rangle), \\ \hat{U}(\pi/2)|L\rangle(\alpha|\uparrow\rangle + \beta|\downarrow\rangle) &= |L\rangle(i\alpha|\uparrow\rangle + \beta|\downarrow\rangle). \end{aligned} \tag{11}$$

In our previous work on this subject,[20] we have discussed the giant optical Faraday rotations induced by a single spin. Here is the reverse process where the giant spin rotations are induced by a single photon (interacting with the spin in the cavity). The speed for this spin rotation is determined by the photon coherence time, which can be several tens of ps.[57] Similarly, two photons in the $|R\rangle_1|R\rangle_2$ or $|L\rangle_1|L\rangle_2$ states can induce 180° spin rotations after their reflections from the cavity with the transformation

$$\begin{aligned} \hat{U}(\pi/2)|R\rangle_1|R\rangle_2(\alpha|\uparrow\rangle+\beta|\downarrow\rangle) &= |R\rangle_1|R\rangle_2(\alpha|\uparrow\rangle-\beta|\downarrow\rangle), \\ \hat{U}(\pi/2)|L\rangle_1|L\rangle_2(\alpha|\uparrow\rangle+\beta|\downarrow\rangle) &= |L\rangle_1|L\rangle_2(-\alpha|\uparrow\rangle+\beta|\downarrow\rangle). \end{aligned} \tag{12}$$

The speed for this spin rotation is determined by the time interval of two photons, which can be in the ns range.[57] Spin rotations with other angles are also possible if we tune the photon frequency to get different phase shift $\Delta\varphi$. The state transformation can be written as

$$\begin{aligned} \hat{U}(\Delta\varphi)|R\rangle(\alpha|\uparrow\rangle + \beta|\downarrow\rangle) &= |R\rangle[\alpha|\uparrow\rangle + e^{i\Delta\varphi}\beta|\downarrow\rangle]. \\ \hat{U}(\Delta\varphi)|L\rangle(\alpha|\uparrow\rangle + \beta|\downarrow\rangle) &= |L\rangle[e^{i\Delta\varphi}\alpha|\uparrow\rangle + \beta|\downarrow\rangle], \end{aligned} \tag{13}$$

and $+\Delta\varphi$ or $-\Delta\varphi$ spin rotations could be performed. N photons (or N passes of a single photon) in the $|R\rangle_1|R\rangle_2\cdots|R\rangle_N$ or $|L\rangle_1|L\rangle_2\cdots|L\rangle_N$ states could be sent to the cavity in sequence and make $+N\Delta\varphi$ or $-N\Delta\varphi$ spin rotations. The phase shift $\Delta\varphi$ is tuneable between $-\pi$ and $+\pi$ by tuning the photon frequency in an ideal system. The range of $\Delta\varphi$ is reduced by the cavity side leakage and the cavity loss as discussed in our previous work.[20] This optical spin manipulation method at single-photon levels is compatible with our schemes and is different from another optical method based on ac Stark effect as demonstrated recently.[72–75]

As discussed above, spin coherence time T_2^e is important as our schemes rely on the coherent photon-spin interaction: (1) The storage time of the spin memory is limited by T_2^e; (2) the entanglement fidelity for the BSA depends on T_2^e by Eq. (10); (3) the time window for the BSA to capture photons is determined by T_2^e. The longer the T_2^e, the bigger the time window, and the stronger the signal rate (or more loss can be resisted). The electron spin coherence time in GaAs-based or InAs-based QD is normally quite short ($T_2^e \sim$ ns)[78,79] due to the hyperfine interaction between the electron spin and 10^4–10^5 host nuclear spins, whereas the electron spin relaxation time is much longer ($T_1^e \sim$ ms)[80,81] due to the suppressed electron-phonon and spin-orbit interactions in QDs. If nuclear spin fluctuations are suppressed,[82] T_2^e can be prolonged with the limit set by $T_2^e \leqslant 2T_1^e$. Isotope engineering techniques[83] are not suitable here as elements In, Ga, and As do not have stable isotopes with zero-spin nuclei. Spin echo techniques have been demonstrated to suppress the nuclear spin fluctuations effectively and prolong the electron spin coherence to the μs range.[75,78,79,84,85] However, our schemes

are not compatible with such ESR-based spin manipulations in an external magnetic field. As discussed above, two single photons can play the role of the π-pulse to make the 180° spin rotation around the optical axis. Therefore we could still apply the spin echo techniques (or dynamical decoupling[86,87]) to protect the spin coherence with various pulse sequences,[88–94] but now using single photon pulses,[95] rather than microwave pulses[78,79] or optical pulses.[75,84,85]

IV. ENTANGLEMENT SWAPPING USING TYPE-I BELL-STATE ANALYZER

As well as state teleportation, the BSA is also the key component for entanglement swapping, dense coding, and fault tolerant quantum computing. As an example, we perform entanglement swapping with the spin-cavity unit (see Fig. 3). We prepare two independent EPR pairs: photon 1,2 in the state $|\psi^{\rm ph}\rangle_{12} = (|R\rangle_1|L\rangle_2 + |L\rangle_1|R\rangle_2)/\sqrt{2}$, and photon 3,4 in the state $|\psi^{\rm ph}\rangle_{34} = (|R\rangle_3|L\rangle_4 + |L\rangle_3|R\rangle_4)/\sqrt{2}$. The spin is initialized to $|\psi^s\rangle = |+\rangle$. Photons 1 and 3 are then targeted to the spin-cavity unit. After the reflection of photons 1 and 3, the total state of four photons with one spin is transformed into

$$
\begin{aligned}
&|\psi^{\rm ph}\rangle_{12} \otimes |\psi^{\rm ph}\rangle_{34} \otimes |\psi^s\rangle \xrightarrow[\text{to photon 1,3}]{\hat{U}(\pi/3)} \\
&\quad \times \tfrac{1}{4}\{[|H\rangle_1|H\rangle_3 - |V\rangle_1|V\rangle_3]|-\rangle[|L\rangle_2|L\rangle_4 - |R\rangle_2|R\rangle_4] \\
&\quad + i[|H\rangle_1|V\rangle_3 + |V\rangle_1|H\rangle_3]|-\rangle[|L\rangle_2|L\rangle_4 + |R\rangle_2|R\rangle_4] \\
&\quad + i[|H\rangle_1|H\rangle_3 + |V\rangle_1|V\rangle_3]|+\rangle[|L\rangle_2|R\rangle_4 + |R\rangle_2|L\rangle_4] \\
&\quad + [|H\rangle_1|V\rangle_3 - |V\rangle_1|H\rangle_3]|+\rangle[|L\rangle_2|R\rangle_4 - |R\rangle_2|L\rangle_4]\}.
\end{aligned} \tag{14}
$$

After the photon polarization and the spin measurements, photons 2 and 4 get entangled in the four Bell states, which are unequivocally associated to the measurement results consisting of polarizations of photons 1 and 3 in the $|H\rangle$, $|V\rangle$ basis and the spin in the $|+\rangle$, $|-\rangle$ basis (see Table II).

As discussed in our previous work,[21] the spin-cavity unit can work as a photon entangler, which generates arbitrary entanglement, including Bell states, GHZ states, and cluster states. Therefore, we think this spin-cavity unit is generally an arbitrary entanglement generator and analyzer. For instance, to

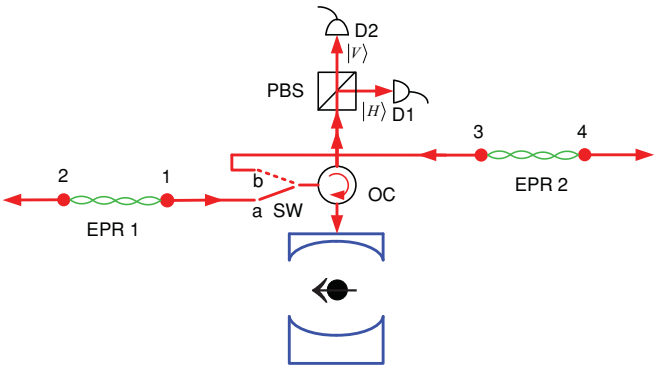

FIG. 3. (Color online) Schematic of entanglement swapping between two EPR pairs with the type-I spin-cavity unit. In this case, the spin-cavity unit works as a four-photon GHZ-state generator and a complete Bell-state analyzer.

TABLE II. The correspondence between the photon 1, 3 polarization and the spin measurement results and the photon 2, 4 Bell states in the case of the entanglement swapping.

Photons 1, 3	Spin	Photons 2, 4
$\|H\rangle_1\|H\rangle_3$ or $\|V\rangle_1\|V\rangle_3$	$\|-\rangle$	$[\|L\rangle_2\|L\rangle_4 - \|R\rangle_2\|R\rangle_4]/\sqrt{2}$
$\|H\rangle_1\|V\rangle_3$ or $\|V\rangle_1\|H\rangle_3$	$\|-\rangle$	$[\|L\rangle_2\|L\rangle_4 + \|R\rangle_2\|R\rangle_4]/\sqrt{2}$
$\|H\rangle_1\|H\rangle_3$ or $\|V\rangle_1\|V\rangle_3$	$\|+\rangle$	$[\|L\rangle_2\|R\rangle_4 + \|R\rangle_2\|L\rangle_4]/\sqrt{2}$
$\|H\rangle_1\|V\rangle_3$ or $\|V\rangle_1\|H\rangle_3$	$\|+\rangle$	$[\|L\rangle_2\|R\rangle_4 - \|R\rangle_2\|L\rangle_4]/\sqrt{2}$

analyze an N-photon GHZ state, we can cascade the Bell-state analysis to get the full information on the state structure. To our knowledge, only a partial GHZ-state analyzer has ever been reported.[96] With the GHZ-state analyzer, our scheme can be extended to quantum teleportation based on multiparticle entanglement.[97]

If we go further, this spin-cavity unit is already a quantum computer as only a quantum computer can generate and identify arbitrary entanglement. The two-qubit phase shift gate described by $\hat{U}(\pi/2)$ is universal when assisted by arbitrary single-qubit gates,[98,99] so all quantum logic operations (including the CNOT gate and CZ gate) can be built from it. Details will be discussed elsewhere.[100]

V. BELL-STATE ANALYZER (TYPE II)

In this section, we consider another type of spin-cavity unit (type II) with a single spin in a double-sided optical microcavity where the top and bottom mirrors are both partially reflective. In this spin-cavity system, GCB manifests as the different reflection and transmission coefficients between $|R\rangle$ and $|L\rangle$ photons. This allows us to make another photon-spin entangling gate-entanglement beam splitter.[22] The transmission and reflection operators for this entanglement beam splitter are defined as

$$
\begin{aligned}
\hat{t}(\omega) &= t_0(\omega)(|R\rangle\langle R| \otimes |\uparrow\rangle\langle\uparrow| + |L\rangle\langle L| \otimes |\downarrow\rangle\langle\downarrow|), \\
\hat{r}(\omega) &= r_h(\omega)(|R\rangle\langle R| \otimes |\downarrow\rangle\langle\downarrow| + |L\rangle\langle L| \otimes |\uparrow\rangle\langle\uparrow|),
\end{aligned} \tag{15}
$$

where $t_0(\omega)$ is the transmission coefficient of the empty (cold) cavity, and $r_h(\omega)$ is the reflection coefficient of the hot cavity. The defined operators $\hat{t}(\omega)$ and $\hat{e}(\omega)$ can work with higher fidelity and efficiency in the strong coupling regime, and lower fidelity and efficiency in the weak coupling regime. If $\omega = \omega_0$ is set, and $\kappa_s \ll \kappa$ and $g^2 \gg \kappa\gamma/2$ (e.g., in the strong coupling regime or the Purcell regime) are met, we get $t_0(\omega_0) \simeq -1$ and $r_h(\omega_0) \simeq 1$. By applying $\hat{r}(\omega_0)$, $\hat{t}(\omega_0)$ to the four Bell states, we find $|\Psi^{\pm}\rangle|+\rangle$ is transformed to

$$
-\left[|R\rangle_1^r|L\rangle_2^r \pm |L\rangle_1^r|R\rangle_2^t\right]|\uparrow\rangle - \left[|R\rangle_1^r|L\rangle_2^t \pm |L\rangle_1^t|R\rangle_2^r\right]|\downarrow\rangle \tag{16}
$$

with one photon reflected and another transmitted, and $|\Phi^{\pm}\rangle|+\rangle$ is transformed to

$$
\left[|R\rangle_1^t|R\rangle_2^t \pm |L\rangle_1^r|L\rangle_2^r\right]|\uparrow\rangle + \left[|R\rangle_1^r|R\rangle_2^r \pm |L\rangle_1^t|L\rangle_2^t\right]|\downarrow\rangle \tag{17}
$$

with two photons both reflected or both transmitted.

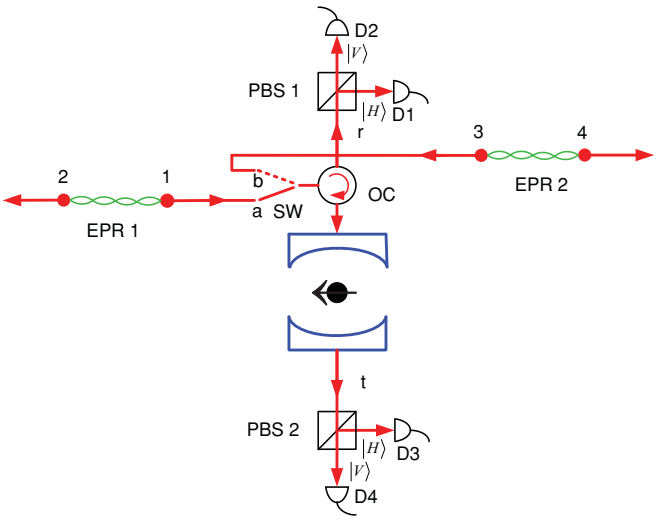

FIG. 4. (Color online) Schematic of entanglement swapping with a QD-spin in a double-sided microcavity (type II). In this case, the entanglement beam splitter works as a five-qubit GHZ-state generator and a complete Bell-state analyzer. This unit can also be used for state teleportation (not shown here). SW (optical switch), OC (optical circulator), PBS 1 and PBS 2 (polarizing beam splitters), D1–D4 (photon detectors).

We can distinguish $|\Psi^{\pm}\rangle$ from $|\Phi^{\pm}\rangle$ by simply discriminating the two photons in the same or different output ports, rather than the spin measurements in the type-I unit. The photon polarization measurement in the $|H\rangle$, $|V\rangle$ basis can distinguish between $|\Psi^{+}\rangle$ and $|\Psi^{-}\rangle$ and between $|\Phi^{+}\rangle$ and $|\Phi^{-}\rangle$. Obviously, the type-II spin-cavity unit is also a complete BSA with a built-in spin memory and can be used for either state teleportation or entanglement swapping (see Fig. 4). Generally, this unit can also generate and analyze arbitrary entanglement as the photon-spin entangling gate described by Eq. (15) is universal together with single-qubit gates.[22,100] Recently, Bonato *et al.* constructed a complete BSA by combining the entanglement beam splitter with an external interferometer.[33] In their configuration, the spin measurement (rather than the port discrimination) is used to distinguish $|\Psi^{\pm}\rangle$ from $|\Phi^{\pm}\rangle$. With no external interferometer included, we think our design is stable and simple.

For type-II BSA, discussions on the fidelity and efficiency are similar to that for entanglement generation that has been presented in our previous work.[22] Both type-I and type-II BSAs can work in the weak and strong coupling regime, but high fidelity and high efficiency can be achieved only when the side leakage and cavity loss is low.

As $t_0(\omega_0) \simeq -1$ and $r_h(\omega_0) \simeq 1$, there is π phase shift between the transmitted and reflected states, which is also recognized by Waks and Vučković.[101] As a result, a single photon in the $|R\rangle$ or $|L\rangle$ state can also induce the 180° spin rotation around the optical axis in the type-II structure, and the spin echo techniques can be applied to preserve the spin coherence as in the type-I structure (see Sec. III). Spin rotations of arbitrary angles are also possible for the type-II spin-cavity unit by placing a tunable phase shifter in the transmission or refection port.

VI. CONCLUSIONS

We have developed schemes for efficient, heralded, and loss-resistant quantum teleportation by exploiting the coherent photon-spin interaction in a spin-cavity QED system. In the ideal case, these schemes are deterministic, but with reduced efficiency when losses are included. State teleportation and entanglement swapping is heralded by the sequential detection (rather than the coincidence measurement) of two photons at different arrival times ($\Delta t < T_2^e$) and is finished after the spin measurement. The spin-cavity unit works as a GHZ-state generator and a complete Bell-state analyzer with a built-in spin memory, but generally it is an arbitrary entanglement generator and analyzer (i.e., a quantum computer). The schemes can thus be extended to teleportation based on multi-particle entanglement. As the spin-cavity unit provides a photon-spin interface,[21,22] efficient teleportation between separated spin qubits in cavities is also possible.

We have shown that these schemes could be realized with current technology. In the weak coupling regime, unity fidelity and <10% efficiency could be achieved. In the strong coupling regime, we expect near-unity fidelity and >35% efficiency (100% efficiency in the ideal case).

We have also proposed schemes for optical spin manipulations at single photon levels by applying the photon-spin entangling gates and schemes for preserving the spin coherence via the spin echo techniques. As the two types of photon-spin entangling gates are universal, the versatile spin-cavity systems can be applied in all aspects of quantum information science and technology, not only for large-scale quantum communication networks, but also for scalable quantum computing with either photons or spins as qubits.

ACKNOWLEDGMENTS

We thank M. Atatüre, S. Bose, S. Popescu, and J.L. O'Brien for helpful discussions. This work is partly funded by QAP (Contract No. EU IST015848) and ERC advanced grant QUOWSS.

*chengyong.hu@bristol.ac.uk

[1]N. Gisin, G. Ribordy, W. Tittel, and H. Zbinden, Rev. Mod. Phys. **74**, 145 (2002).
[2]C. H. Bennett, G. Brassard, C. Crépeau, R. Jozsa, A. Peres, and W. K. Wootters, Phys. Rev. Lett. **70**, 1895 (1993).
[3]M. Zukowski, A. Zeilinger, M. A. Horne, and A. K. Ekert, Phys. Rev. Lett. **71**, 4287 (1993).
[4]J. I. Cirac, P. Zoller, H. J. Kimble, and H. Mabuchi, Phys. Rev. Lett. **78**, 3221 (1997).
[5]H. J. Kimble, Nature (London) **453**, 1023 (2008).
[6]H.-J. Briegel, W. Dür, J. I. Cirac, and P. Zoller, Phys. Rev. Lett. **81**, 5932 (1998).
[7]W. Dür, H.-J. Briegel, J. I. Cirac, and P. Zoller, Phys. Rev. A **59**, 169 (1999).

[8]L.-M. Duan, M. D. Lukin, J. I. Cirac, and P. Zoller, Nature (London) **414**, 413 (2001).
[9]L. Childress, J. M. Taylor, A. S. Sørensen, and M. D. Lukin, Phys. Rev. Lett. **96**, 070504 (2006).
[10]B. Zhao, Z.-B. Chen, Y.-A. Chen, J. Schmiedmayer, and J.-W. Pan, Phys. Rev. Lett. **98**, 240502 (2007).
[11]P. van Loock, T. D. Ladd, K. Sanaka, F. Yamaguchi, K. Nemoto, W. J. Munro, and Y. Yamamoto, Phys. Rev. Lett. **96**, 240501 (2006).
[12]W. J. Munro, R. Van Meter, Sebastien, G. R. Louis, and K. Nemoto, Phys. Rev. Lett. **101**, 040502 (2008).
[13]E. Waks, A. Zeevi, and Y. Yamamoto, Phys. Rev. A **65**, 052310 (2002).
[14]B. C. Jacobs, T. B. Pittman, and J. D. Franson, Phys. Rev. A **66**, 052307 (2002).
[15]D. Collins, N. Gisin, and H. D. Riedmatten, J. Mod. Opt. **52**, 735 (2005).
[16]C. K. Hong, Z. Y. Ou, and L. Mandel, Phys. Rev. Lett. **59**, 2044 (1987).
[17]D. Bouwmeester, J.-W. Pan, K. Mattle, M. Eibl, H. Weinfurter, and A. Zeilinger, Nature (London) **390**, 575 (1997).
[18]H. de Riedmatten, I. Marcikic, W. Tittel, H. Zbinden, D. Collins, and N. Gisin, Phys. Rev. Lett. **92**, 047904 (2004).
[19]J.-W. Pan, D. Bouwmeester, H. Weinfurter, and A. Zeilinger, Phys. Rev. Lett. **80**, 3891 (1998).
[20]C. Y. Hu, A. Young, J. L. O'Brien, W. J. Munro, and J. G. Rarity, Phys. Rev. B **78**, 085307 (2008).
[21]C. Y. Hu, W. J. Munro, and J. G. Rarity, Phys. Rev. B **78**, 125318 (2008).
[22]C. Y. Hu, W. J. Munro, J. L. O'Brien, and J. G. Rarity, Phys. Rev. B **80**, 205326 (2009).
[23]A deterministic and nondestructive CNOT gate can be built from the photon-spin entangling gate $\hat{U}(\pi/2)$ (see Ref. 21). It is well known that the CNOT gate is universal and can be used for entanglement purification. However, the CNOT-based purification can be simplified by directly using the gate $\hat{U}(\pi/2)$ that is also universal (see Ref. 100). Therefore, the spin-cavity unit can work as a full quantum repeater (see Ref. 6) that combines entanglement swapping, entanglement purification, and quantum memory. Quantum communications over arbitrary long distance are possible with quantum repeaters.
[24]J. Calsamiglia and N. Lütkenhaus, Appl. Phys. B**72**, 67 (2001).
[25]Y.-H. Kim, S. P. Kulik, and Y. Shih, Phys. Rev. Lett. **86**, 1370 (2001).
[26]E. Knill, R. Laflamme, and G. Milburn, Nature (London) **409**, 46 (2001).
[27]D. Boschi, S. Branca, F. De Martini, L. Hardy, and S. Popescu, Phys. Rev. Lett. **80**, 1121 (1998).
[28]P. G. Kwiat and H. Weinfurter, Phys. Rev. A **58**, R2623 (1998).
[29]S. P. Walborn, S. Pádua, and C. H. Monken, Phys. Rev. A **68**, 042313 (2003).
[30]C. Schuck, G. Huber, C. Kurtsiefer, and H. Weinfurter, Phys. Rev. Lett. **96**, 190501 (2006).
[31]M. Barbieri, G. Vallone, P. Mataloni, and F. De Martini, Phys. Rev. A **75**, 042317 (2007).
[32]J. T. Barreiro, T. Wei, and P. G. Kwiat, Nature Phys. **4**, 282 (2008).
[33]C. Bonato, F. Haupt, S. S. R. Oemrawsingh, J. Gudat, D. Ding, M. P. van Exter, and D. Bouwmeester, Phys. Rev. Lett. **104**, 160503 (2010).
[34]L.-M. Duan and H. J. Kimble, Phys. Rev. Lett. **92**, 127902 (2004).
[35]Q. A. Turchette, C. J. Hood, W. Lange, H. Mabuchi, and H. J. Kimble, Phys. Rev. Lett. **75**, 4710 (1995).
[36]A. Imamoglu, H. Schmidt, G. Woods, and M. Deutsch, Phys. Rev. Lett. **79**, 1467 (1997).
[37]K. M. Gheri, K. Ellinger, T. Pellizzari, and P. Zoller, Fortschr. Phys. **46**, 401 (1998).
[38]K. Koshino, S. Ishizaka, and Y. Nakamura, Phys. Rev. A **82**, 010301(R) (2010).
[39]M. Greenberger, M. A. Horne, A. Shimony, and A. Zeilinger, Am. J. Phys. **58**, 1131 (1990).
[40]We assume ∼5 ps photon pulses and ∼100 GHz repetition rate to achieve the maximum enhancement.
[41]T. Schmitt-Manderbach *et al.*, Phys. Rev. Lett. **98**, 010504 (2007).
[42]A. Fedrizzi, R. Ursin, T. Herbst, M. Nespoli, R. Prevede, T. Scheidl, F. Tiefenbacher, T. Jennewein, and A. Zeilinger, Nature Phys. **5**, 389 (2009).
[43]Xian-Min Jin *et al.*, Nature Photon. **4**, 376 (2010).
[44]M. Aspelmeyer, M. Pfennigbauer, W. R. Leeb, and A. Zeilinger, IEEE J. Sel. Top. Quantum Electron. **9**, 1541 (2003).
[45]M. T. Rakher, N. G. Stoltz, L. A. Coldren, P. M. Petroff, and D. Bouwmeester, Phys. Rev. Lett. **102**, 097403 (2009).
[46]I. Fushman, D. Englund, A. Faraon, N. Stoltz, P. Petroff, and J. Vučković, Science **320**, 769 (2008).
[47]The reflection operator $\hat{r}$ defined by Eq. (6) is rigorous and does not require the weak excitation approximation. Any approximation just affects the expressions of $r_0(\omega)$ and $r_h(\omega)$.
[48]J. M. Raimond, M. Brune, and S. Haroche, Rev. Mod. Phys. **73**, 565 (2001).
[49]The solutions of the equation $\varphi_h(\omega) - \varphi_0(\omega) = \pm\pi/2$ depend on the values of $g/(\kappa + \kappa_s)$ and κ_s/κ, and are twofold degenerate with the positive and negative frequency detunings. For $\kappa_s/\kappa < 1.0$, there are six solutions at most. For $1.0 \leqslant \kappa_s/\kappa \leqslant 1.3$, there are four solutions at most. For $\kappa_s/\kappa > 1.3$, there is no solution. In our previous work (Refs. 20 and 21), we discussed two solutions that lie closest to the central frequency in the strong coupling limit with $g/(\kappa + \kappa_s) \geqslant 1.5$, and yield the highest fidelity and efficiency. In Fig. 2, we present all solutions in both the strong and the weak coupling regime.
[50]J. P. Reithmaier, G. Sęk, A. Löffler, C. Hofmann, S. Kuhn, S. Reitzenstein, L. V. Keldysh, V. D. Kulakovskii, T. L. Reinecke, and A. Forchel, Nature (London) **432**, 197 (2004).
[51]T. Yoshie, A. Scherer, J. Hendrickson, G. Khitrova, H. M. Gibbs, G. Rupper, C. Ell, O. B. Shchekin, and D. G. Deppe, Nature (London) **432**, 200 (2004).
[52]E. Peter, P. Senellart, D. Martrou, A. Lemaître, J. Hours, J. M. Gérard, and J. Bloch, Phys. Rev. Lett. **95**, 067401 (2005).
[53]S. Reitzenstein, C. Hofmann, A. Gorbunov, M. Strauß, S. H. Kwon, C. Schneider, A. Löffler, S. Höfling, M. Kamp, and A. Forchel, Appl. Phys. Lett. **90**, 251109 (2007).
[54]In the laboratory, we have recently achieved $g/(\kappa_s + \kappa) \geqslant 1.2$ for a $d = 2.5\,\mu$m micropillar microcavity containing self-assembled In(Ga)As/GaAs QDs, and we have seen phase shifts up to 0.1 radian limited primarily by the side leakage and cavity loss. A. B. Young *et al.*, e-print arXiv:1011.0384.
[55]Here g and κ can be controlled independently as g is determined by the trion oscillator strength and the cavity modal volume, whereas κ by the cavity quality factor only.
[56]V. Loo, L. Lanco, A. Lemaître, I. Sagnes, O. Krebs, P. Voisin, and P. Senellart, Appl. Phys. Lett. **97**, 241110 (2010).

[57]By taking $g/(\kappa+\kappa_s)=1.0$, $\kappa_s/\kappa=0.7$, and $\gamma/\kappa=0.1$, which are experimentally achievable for a $d=1.5\,\mu$m micropillar microcavity with $Q=1.7\times10^4$ (see the text), we get the critical photon number $n_0=2\times10^{-3}$ and the cavity lifetime $\tau=9$ ps. Therefore the time interval between two photons should be longer than $\tau/n_0=4.5$ ns to make the weak excitation approximation valid. Note that the photon coherence time should be longer than the cavity lifetime so that the phase shift can be well defined (Ref. 21).

[58]H. J. Kimble, in *Cavity Quantum Electrodynamics*, edited by P. Berman (Academic Press, San Diego, 1994).

[59]P. Borri, W. Langbein, S. Schneider, U. Woggon, R. L. Sellin, D. Ouyang, and D. Bimberg, Phys. Rev. Lett. **87**, 157401 (2001).

[60]D. Birkedal, K. Leosson, and J. M. Hvam, Phys. Rev. Lett. **87**, 227401 (2001).

[61]W. Langbein, P. Borri, U. Woggon, V. Stavarache, D. Reuter, and A. D. Wieck, Phys. Rev. B **70**, 033301 (2004).

[62]J. Fischer, W. A. Coish, D. V. Bulaev, and D. Loss, Phys. Rev. B **78**, 155329 (2008).

[63]C. Testelin, F. Bernardot, B. Eble, and M. Chamarro, Phys. Rev. B **79**, 195440 (2009).

[64]D. Heiss, S. Schaeck, H. Huebl, M. Bichler, G. Abstreiter, J. J. Finley, D. V. Bulaev, and D. Loss, Phys. Rev. B **76**, 241306(R) (2007).

[65]B. D. Gerardot, D. Brunner, P. A. Dalgarno, P. Öhberg, S. Seidl, M. Kroner, K. Karrai, N. G. Stoltz, P. M. Petroff, and R. J. Warburton, Nature (London) **451**, 441 (2008).

[66]D. Brunner, B. D. Gerardot, P. A. Dalgarno, G. Wüst, K. Karrai, N. G. Stoltz, P. M. Petroff, and R. J. Warburton, Science **325**, 70 (2009).

[67]G. Bester, S. Nair, and A. Zunger, Phys. Rev. B **67**, 161306(R) (2003).

[68]M. Bayer *et al.*, Phys. Rev. B **65**, 195315 (2002).

[69]J. J. Finley, D. J. Mowbray, M. S. Skolnick, A. D. Ashmore, C. Baker, A. F. G. Monte, and M. Hopkinson, Phys. Rev. B **66**, 153316 (2002).

[70]M. Atatüre, J. Dreiser, A. Badolato, A. Hogele, K. Karrai, and A. Imamoglu, Science **312**, 551 (2006).

[71]Xiaodong Xu, Yanwen Wu, Bo Sun, Qiong Huang, Jun Cheng, D. G. Steel, A. S. Bracker, D. Gammon, C. Emary, and L. J. Sham, Phys. Rev. Lett. **99**, 097401 (2007).

[72]J. A. Gupta, R. Knobel, N. Samarth, and D. D. Awschalom, Science **292**, 2458 (2001).

[73]J. Berezovsky, M. H. Mikkelsen, N. G. Stoltz, L. A. Coldren, and D. D. Awschalom, Science **320**, 349 (2008).

[74]D. Press, T. D. Ladd, B. Zhang, and Y. Yamamoto, Nature (London) **456**, 218 (2008).

[75]A. Greilich, S. E. Economou, S. Spatzek, D. R. Yakovlev, D. Reuter, A. D. Wieck, T. L. Reinecke, and M. Bayer, Nature Phys. **5**, 262 (2009).

[76]B. Misra and E. C. G. Sudarshan, J. Math. Phys. **18**, 756 (1977).

[77]W. M. Itano, D. J. Heinzen, J. J. Bollinger, and D. J. Wineland, Phys. Rev. A **41**, 2295 (1990).

[78]J. R. Petta, A. C. Johnson, J. M. Taylor, E. A. Laird, A. Yacoby, M. D. Lukin, C. M. Marcus, M. P. Hanson, and A. C. Gossard, Science **309**, 2180 (2005).

[79]F. H. L. Koppens, K. C. Nowack, and L. M. K. Vandersypen, Phys. Rev. Lett. **100**, 236802 (2008).

[80]J. M. Elzerman, R. Hanson, L. H. Willems van Beveren, B. Witkamp, L. M. K. Vandersypen, and L. P. Kouwenhoven, Nature (London) **430**, 431 (2004).

[81]M. Kroutvar, Y. Ducommun, D. Heiss, M. Bichler, D. Schuh, G. Abstreiter, and J. J. Finley, Nature (London) **432**, 81 (2004).

[82]Even if the nuclear-spin induced decoherence is removed by using the isotope engineering or spin-echo techniques, there still exists other decoherence channels in an individual QD, e.g., the decoherence processes due to the electron-phonon and spin-orbit interactions, which could be reduced by engineering the QD shape, size, or confinement, lowering the temperature, and so on. For a review, see, e.g., J. Fischer and D. Loss, Science **324**, 1277 (2009).

[83]G. Balasubramanian *et al.*, Nat. Mater. **8**, 383 (2009).

[84]S. M. Clark, K.-M. C. Fu, Q. Zhang, T. D. Ladd, C. Stanley, and Y. Yamamoto, Phys. Rev. Lett. **102**, 247601 (2009).

[85]D. Press, K. De Greve, P. L. McMahon, T. D. Ladd, B. Friess, C. Schneider, M. Kamp, S. Höfling, A. Forchel, and Y. Yamamoto, Nature Photon. **4**, 367 (2010).

[86]L. Viola and S. Lloyd, Phys. Rev. A **58**, 2733 (1998).

[87]L. Viola, E. Knill, and S. Lloyd, Phys. Rev. Lett. **82**, 2417 (1999).

[88]E. L. Hahn, Phys. Rev. **80**, 580 (1950).

[89]H. Y. Carr and E. M. Purcell, Phys. Rev. **94**, 630 (1954).

[90]S. Meiboom and D. Gill, Rev. Sci. Instrum. **29**, 688 (1958).

[91]K. Khodjasteh and D. A. Lidar, Phys. Rev. Lett. **95**, 180501 (2005).

[92]W. Yao, R. B. Liu, and L. J. Sham, Phys. Rev. Lett. **98**, 077602 (2007).

[93]W. M. Witzel and S. Das Sarma, Phys. Rev. B **76**, 241303(R) (2007).

[94]G. S. Uhrig, Phys. Rev. Lett. **98**, 100504 (2007).

[95]The single-photon based spin echoes are described in the laboratory reference frame, whereas the ESR-based spin echoes are usually described in the rotating reference frame.

[96]J.-W. Pan and A. Zeilinger, Phys. Rev. A **57**, 2208 (1998).

[97]S. Bose, V. Vedral, and P. L. Knight, Phys. Rev. A **57**, 822 (1998).

[98]A. Barenco, C. H. Bennett, R. Cleve, D. P. DiVincenzo, N. Margolus, P. Shor, T. Sleator, J. A. Smolin, and H. Weinfurter, Phys. Rev. A **52**, 3457 (1995).

[99]S. Lloyd, Phys. Rev. Lett. **75**, 346 (1995).

[100]C. Y. Hu *et al.* (unpublished).

[101]E. Waks and J. Vučković, Phys. Rev. Lett. **96**, 153601 (2006).